European Review for Medical and Pharmacological Sciences 2022; 26: 4638-4653

Evaluation of miR-429 as a novel serum biomarker for pancreatic ductal adenocarcinoma and analysis its tumor suppressor function and target genes

W.-T. HUANG, T.-S. LIN, J.-Y. WU, J.-M. HONG, Y.-L. CHEN, F.-N. QIU

Department of Hepatobiliary Surgery, Fujian Provincial Hospital, Shengli Clinical Medical College of Fujian Medical University, Fuzhou, China

Abstract. – OBJECTIVE: Pancreatic ductal adenocarcinoma (PDAC) is one of the most lethal types of cancer. Various microRNAs have been identified to play an important role in PDAC. The study aimed to explore the role of miR-429 in PDAC.

PATIENTS AND METHODS: The expression and prognostic value of miR-429 were first analyzed using The Cancer Genome Atlas (TCGA) and Gene Expression Omnibus (GEO) databases. Next, miR-429 expression was evaluated in the tissues and serum of 90 patients with PDAC. CCK8, SRB, wound healing and transwell assays were used to determine the effect of miR-429 on the proliferation, invasion, and migration of PDAC cells, respectively. Weighted gene co-expression network analysis (WGCNA), correlation analysis, TargetScan, and miRDB databases were used to screen and identify the target genes of miR-429.

RESULTS: The results revealed that the expression of miR-429 was downregulated in PDAC tissues and the serum compared with those in normal tissues and the serum of healthy volunteers, respectively. The decreased expression of miR-429 was significantly associated with shorter overall survival. The overexpression of miR-429 significantly inhibited the proliferation, invasion, and migration of PDAC cells. Potential target genes of miR-429 were identified using WGCNA and bioinformatics analysis, and the results showed that cadherin 11 (CDH11), inositol polyphosphate-4-phosphatase type I (INPP4A), laminin gamma 1 (LAMC1), low density lipoprotein receptor-related protein 1 (LRP1), and quaking (QKI) were potential target genes of miR-429 in PDAC. Lower expression of CDH11 and QKI was associated with a more favorable prognosis in patients with PDAC. The overexpression of miR-429 could inhibit the expression of CDH11 and QKI. A nomogram model, involving miR-429, CDH11, and QKI, was subsequently constructed to determine their ability to accurately predict overall and disease-free survival in patients with PDAC.

CONCLUSIONS: Taken together, miR-429 is involved in the development and progress of PDAC. MiR-429 could be recommended as a prognostic biomarker and therapeutic indicator in PDAC diagnosis.

Key Words:
MicroRNA-429, PDAC, CDH11, QKI, Biomarker.

Abbreviations

PDAC: Pancreatic ductal adenocarcinoma; WGCNA: Weighted gene co-expression network analysis; OS: overall survival; DFS: disease-free survival; CDH11: cadherin 11; INPP4A: inositol polyphosphate-4-phosphatase type I; LAMC1: laminin gamma 1; LRP1: low density lipoprotein receptor-related protein 1; QKI: Quaking; GC: gastric cancer; BC: breast cancer; EC: esophageal cancer; GBM: glioblastoma; EmCa: endometrial cancer; LC: lung cancer; BP: biological processes; CC: cellular components; MF: molecular function enrichment; DEGs: differentially expressed genes; TCGA: The Cancer Genome Atlas; GEO: Gene Expression Omnibus; RPMI-1640: Roswell Park Memorial Institute Medium; KEGG: Kyoto Encyclopedia of Genes and Genomes; CCK-8: Cell Counting Kit-8; SRB: Sulforhodamine B.

Introduction

Pancreatic cancer (PC) is one of the common types of malignant tumor of the digestive tract. The clinical symptoms of pancreatic cancer are insidious and atypical. Thus, the disease is difficult to diagnose and treat. In total, about 90% of pancreatic cancer cases are the pancreatic ductal adenocarcinoma (PDAC) subtype, and its morbidity and mortality have continued to significantly increase in recent years[1-3]. In addition, as

Corresponding Author: Wentao Huang, MD, e-mail: drhuangwt@fjmu.edu.cn

the pancreas is located behind the peritoneum and the early symptoms of PDAC are not evident, it is very difficult to diagnose PDAC early. Thus, the majority of patients with PDAC have reached the locally advanced stage at the time of diagnosis, or their tumors are unresectable or have undergone distant metastases. Unfortunately, this means that a large percentage of patients with PDAC are diagnosed at the advanced stage of the disease, and the median survival time for these patients is only 6-12 months[4-6].

MicroRNAs (miRNAs/miRs) play an important role in the regulation of gene expression and the progression of numerous types of tumors[7-9]. Under pathological conditions, the development of different types of cancer has been discovered to be accompanied by the aberrant expression of specific miRNAs. Previous studies[10-13] have reported that miR-429 functioned as either a pro-oncogenic factor or tumor suppressor in different types of tumors. For example, miR-429 was found to act as a tumor suppressor in gastric cancer (GC)[10], breast cancer (BC)[11], esophageal cancer[12], and PDAC[13]. However, other studies[14,15] have demonstrated that miR-429 exerted tumor-promoting effects in endometrial cancer (EmCa)[14] and lung cancer (LC)[15].

The present study aimed to determine the expression of miR-429 in patients with PDAC. The expression and prognostic value of miR-429 were determined using data from The Cancer Genome Atlas (TCGA) database and tissue samples from 90 patients with PDAC. In addition, the potential of miR-429 to act as a serum biomarker for PDAC screening was assessed. The effect of miR-429 on the proliferation, invasion, and migration of PDAC cells was also analyzed. Furthermore, weighted gene co-expression network analysis (WGCNA) and correlation analysis were used to screen the target genes of miR-429 and explore the possible regulatory mechanisms of miR-429 in PDAC.

Patients and Methods

Clinical Samples

The current study included 90 patients with PDAC who were confirmed by pathology and were admitted to the Department of Hepatobiliary Surgery, Fujian Provincial Hospital (Fuzhou, China) between June 1, 2015 and August 30, 2019. The adjacent non-tumor (1 cm from the cancer tissue boundary) and tumor samples were collected during surgery. Serum samples from patients with PDAC and healthy volunteers were also collected from Fujian Provincial Hospital. A total of 15 healthy volunteers who undertook a routine physical examination were included as healthy volunteers. The following inclusion criteria were used: (1) patients aged 18-80 years; (2) an Eastern Cooperative Oncology Group performance status score of 0-1[16]; (3) patients who had undergone surgical resection as the primary treatment; (4) patients with PDAC who were confirmed histologically or cytologically. The following exclusion criteria were used: (1) patients who had received prior chemotherapy or immunotherapy; (2) patients with concurrent malignancies other than PDAC; (3) patients with serious, unmanageable medical conditions; (4) patients with psychiatric disorders that would limit their ability to meet the study requirements.

Human Ethics Approval and Informed Consent

The study was approved by the Ethics Committee of Fujian Provincial Hospital, Fujian Medical University (approval No. K2014-11-029) and was conducted by the principles of the Declaration of Helsinki. All the PDAC patients and healthy volunteers signed an informed consent document.

Bioinformatics Analysis

The expression of miR-429 and other clinical variables were extracted from The Cancer Genome Atlas (TCGA) (http://www.cbioportal.org/data_sets.jsp) and Gene Expression Omnibus (GEO) databases (http://www.ncbi.nlm.nih.gov/geo/). The following datasets containing data on patients with PDAC were collected from the GEO database: GSE41369[17], GSE71533[18], GSE60979[19], GSE71989[20], GSE91035[21], and GSE24279[22]. The probe ID was converted into a gene symbol first. When a gene was mapped to different probes, the genic expression value was calculated by the average expression value. The GSE41369, GSE71533, and GSE24279 datasets were used to obtain the expression levels of miR-429. The GSE60979, GSE71989, and GSE91035 datasets were used to detect the expression of potential target genes of miR-429.

TargetScan (http://www.Targetscan.org)[23] and miRDB (http://mirdb.org) databases were used to predict potential target genes of miR-429. Gene accession numbers of potential target genes of miR-429 are listed in the **Supplementary Table I**. The Gene Expression Profiling Inter-

active Analysis (GEPIA) database (http://gepia.cancer-pku.cn/index.html) was used to determine the expression of genes in PDAC[24]. Gene Ontology (GO) biological processes (BP), GO cellular components and GO molecular function, and Kyoto Encyclopedia of Genes and Genomes (KEGG) signaling pathway enrichment analyses were performed through the Database for Annotation, Visualization and Integrated Discovery (DAVID; https://david.ncifcrf.gov)[25]. A nomogram was plotted using Hiplot (https://hiplot.com.cn).

Cell Lines and Culture

Bxpc-3 cells (a human pancreatic cancer cell line) were purchased from the American Type Culture Collection. The cells were cultured in Roswell Park Memorial Institute Medium (RPMI-1640) medium (Invitrogen, Carlsbad, CA, USA) supplemented with 10% FBS (Gibco, Waltham, MA, USA), and maintained in a humidified atmosphere at 37°C with 5% CO_2.

Reverse Transcription-Quantitative PCR (RT-qPCR)

Mirna was extracted using RNAiso for Small RNA reagent (Takara, Dalian, China), and reverse transcribed into cDNA using a Mir-X™ miRNA First-Strand Synthesis kit (Takara, Dalian, China). qPCR was subsequently performed to detect gene expression using an SYBR Green Master Mix (Takara, Dalian, China.) on a LightCycler® 480 instrument (Roche Diagnostics, Mannheim, Germany). The following thermocycling conditions were used for qPCR: Initial denaturation at 95°C for 5 sec, followed by 40 cycles of 95°C for 5 sec and 60°C for 30 sec; and dissociation at 95°C for 60 sec, 55˚C for 1 min and 95°C for 30 sec. The primer sequences were showed as follows: MiR-429 sense primer 5'-TAATACTGTCTGGTAAAACCGT-3' and U6 sense primer 5'-CTCGCTTCGGCAGCACA-3'. The miRNA universal antisense primer used for qPCR was included in the Mir-X miRNA First-Strand Synthesis kit. U6 was used as the loading control.

Cell Transfection

To overexpress or silence miR-429, Bxpc-3 cells were transfected with a miR-429 mimic (5'-UAAUACUGUCUGGUAAAACCGU-3') or miR-429 inhibitor (5'-ACGGUUUUACCAGACAGUAUUA-3'), respectively, or a miRNA-negative control (NC) (5'-UGAAUUAGAUGGCGAUGUUUU-3') (GenePharma, Shanghai, China) using Lipofectamine® 2000 reagent (Invitrogen, Carlsbad, CA, USA). Briefly, 50 nM miR-429 mimic, miR-429 inhibitor, or miRNA-NC were added to the diluted Lipofectamine 2000 reagent for 20 min, which was subsequently used to transfect Bxpc-3 cells at ~70% confluence. The cells were cultured at 37°C for 6 h, after which the medium was replaced, and the cells were cultured at 37°C for a further 24 h.

Cell Proliferation Assays

The transfected Bxpc-3 cells were seeded at a density of 5×10^3 cells/well and cultured for 24, 48, or 72 h. Cell proliferation was subsequently detected using Sulforhodamine B (SRB) and Cell Counting Kit-8 (CCK-8) assays[26].

For the SRB assay, the cells were fixed with 3.3% trichloroacetic acid for 1 h. After removing the fixative solution, the cells were incubated with 100 µl SRB (Sigma-Aldrich, Shanghai, China) for 10 min. The cells were then rinsed four times with 1% acetic acid and dried. Stained cells were subsequently dissolved in 100 µl Tris (10 mM) for 10 min under gentle agitation and the absorbance was measured at a wavelength of 490 nm using a microplate reader.

A CCK-8 assay was used to determine cell proliferation. Briefly, 24, 48, or 72 h post-transfection, 10 µl CCK-8 reagent (Transgen, Beijing, China) was added to the plates and incubated at 37°C for 1 h. The absorbance was measured at a wavelength of 450 nm using a microplate reader.

Cell Migration Assay

Transfected Bxpc-3 cells were seeded at a density of $5x10^4$ cells/ well and cultured for 24 h. Serum-free medium was used in the wound healing experiment. Following the incubation, a 10-µl pipette tip was used to create an artificial wound by scratching the cell monolayer. Wound healing was observed after 24 h.

Cell Invasion Assay

Transfected Bxpc-3 cells were seeded into the upper chamber of a Transwell plate. The medium was added to the lower chamber and the cells were cultured at 37°C for 24 h. Following the incubation, the cells were fixed with methanol for 30 min and stained with crystal violet for 20 min.

WGCNA Analysis

WGCNA is a common algorithm for building gene co-expression networks and is performed *via* the WGCNA R package (https://

cran.r-project.org/package=WGCNA). First, the correlation of all genes was calculated to construct the similarity matrix. Next, appropriate soft-thresholding power β was selected to improve co-expression similarity and scale-free topology was implemented. Finally, the adjacency of genes was converted to a topological overlap matrix (TOM), and the corresponding dissimilarity was calculated. Average linkage hierarchical clustering was conducted with TOM-based dissimilarity measurements. The minimum size of the gene dendrogram was 20 and the parameter merge-cut-height was set at 0.25 to merge highly correlated modules.

Statistical Analysis

Statistics were performed using Prism 5.0 software (GraphPad, San Diego, CA, USA). Unpaired Student's *t*-test was done to compare only 2 groups and paired Student's *t*-test was used for 2 paired-groups experiments. 3 group comparisons were performed using Tukey one-way ANOVA. Kaplan-Meier survival curves were used to calculate the survival rate. Each experiment was performed with three replicates and was repeated in triplicate. A $p<0.05$ was considered to indicate a statistically significant difference.

Results

Downregulated MiR-429 Expression is Associated with Poor Prognosis in Patients with PDAC

To determine the expression and prognostic value of miR-429 in PDAC, the TCGA database and two related GEO datasets (GSE41369 and GSE71533) were used. The dataset obtained from TCGA contained 174 PDAC tissues. The GSE41369 dataset contained 9 PDAC and adjacent normal tissues, and the GSE71533 dataset comprised 72 PDAC tissues and 16 adjacent normal tissues. The results revealed that miR-429 expression was downregulated in PDAC tissues compared with that in normal tissues in the GSE41369 and GSE71533 datasets (Figure 1A-B). In addition, the clinical significance of miR-429 in predicting the prognosis of patients with PDAC was determined based on data from the TCGA database. The brief information of these patients was listed in Table I. The results demonstrated that the downregulated expression of miR-429 was associated with a poorer OS and DFS for patients with PDAC (Figure 1C-D).

Univariate and multivariate analyses were performed to determine the predictors for OS and DFS for patients with PDAC. The results of the univariate analysis found that downregulated expression levels

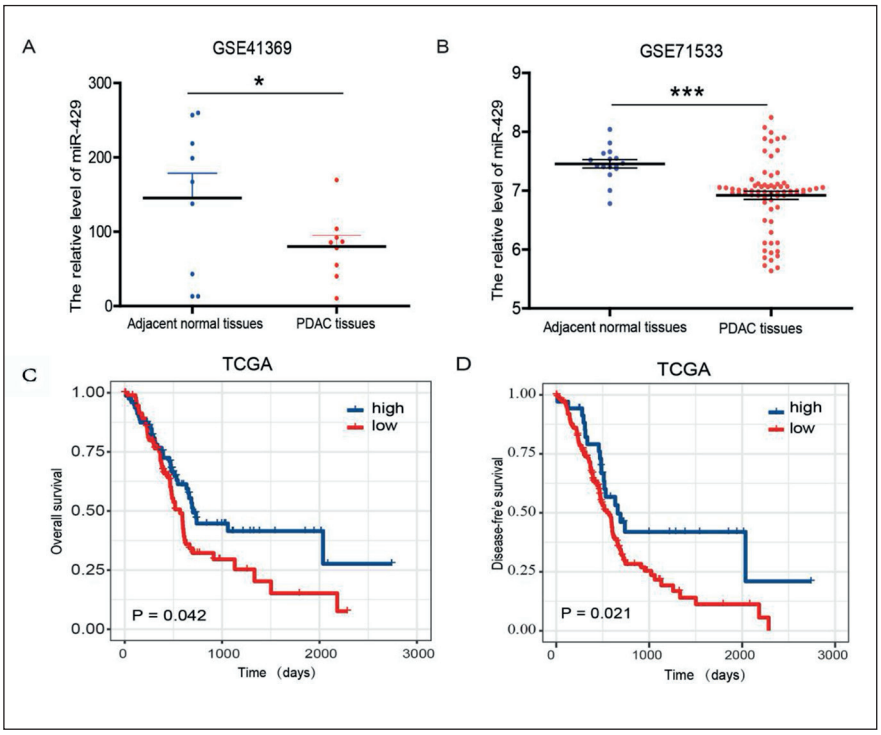

Figure 1. Downregulation of miR-429 was associated with poor prognosis in PDAC patients based on TCGA and GEO database. **A-B,** The expression of miR-429 in PDAC patients based on GSE41369 (**A**) (paired *t*-test) and GSE71533 (**B**) (paired *t*-test). **C-D**, Overall analysis for the prognostic value of miR-429 expression for OS (**C**) and DFS (**D**) in PDAC patients by Kaplan-Meier analysis. The Kaplan-Meier method was used to draw survival curves, and the log-rank test was performed to evaluate survival difference with the best cut-off value. *, $p<0.05$; ***, $p<0.001$.

Table I. Cox PH regression model estimates for the risk of clinical recurrence.

Variable	Age		Stage				Grade			
	≤ 60	> 60	I	II	III	IV	1	2	3	4
N	57	117	20	144	3	4	31	92	47	2
Female	27	53	11	63	2	3	15	46	17	1
Male	30	64	9	81	1	1	16	46	30	1

of miR-429 were associated with poor OS and DFS in patients with PDAC (Table II). Furthermore, to evaluate the independent effect of miR-429 expression levels on OS and DFS, a multivariate Cox regression model was used. The results demonstrated that downregulated miR-429 expression levels were an independent poor prognostic factor for OS and DFS for patients with PDAC (Table III).

Moreover, miR-429 expression was further validated to be downregulated and associated with poor prognosis in 90 patients with PDAC (Figure 2A-B). Detailed miR-429 expression and clinical information for 90 PDAC patients were presented in **Supplementary Table II**.

The Expression of MiR-429 is Decreased in the Serum of Patients with PDAC

Next, the expression of miR-429 in the serum was determined based on data from the GSE24279 dataset. The results revealed that the expression of miR-429 was significantly downregulated in the serum of patients with PDAC compared with those in healthy donors (Figure 3A), and the area under the curve was 0.689 (Figure 3C). In addition, miRNA was extracted from the serum samples of 15 patients with PDAC and 15 healthy donors and was subjected to RT-PCR to analyze the expression of miR-429. The results revealed that miR-429 was also downregulated in the serum of patients with PDAC (Figure 3B-D). Detailed serum miR-429 expression and clinical information for 15 patients and 15 healthy donors were presented in the **Supplementary Table III**. These results suggested that miR-429 expression may be significantly downregulated in the serum of patients with PDAC compared with that in healthy donors.

Table II. Univariate Cox proportional hazard model for OS and DFS in PDAC patients.

Variables	OS		DFS	
	HR (95% CI)	p^a	HR (95% CI)	p^a
Age (years)				
≤ 60	1.423 (0.909-2.228)	0.123	1.456 (0.965-2.196)	0.074
> 60	Reference		Reference	
Sex				
Male	1.215 (0.808-1.826)	0.35	1.176 (0.81-1.708)	0.395
Female	Reference		Reference	
Stage				
I&II	1.405 (0.664-2.972)	0.374	1.745 (0.896-3.395)	0.101
III&IV	Reference		Reference	
Grade				
1&2	1.495 (0.973-2.295)	0.066	1.319 (0.882-1.972)	0.177
3&4	Reference		Reference	
Race				
White	0.888 (0.484-1.632)	0.703	0.783 (0.438-1.40)	0.41
Other	Reference		Reference	
miR-429				
Low	1.54 (1.016-2.335)	0.042	1.802 (1.094-2.968)	0.021
High	Reference		Reference	

Abbreviation: CI, confidence interval; HR, hazard ratio; OS, overall survival; DFS, disease free survival.

Table III. Multivariate Cox proportional hazard model l for OS and DFS in PDAC patients.

Variables	OS		DFS	
	HR (95% CI)	*p*	HR (95% CI)	*p*
Age (years)				
≤ 60	N/A		N/A	
> 60				
Sex				
Male	N/A		N/A	
Female				
Stage				
I&II	N/A		N/A	
III&IV				
Grade				
1&2	N/A		N/A	
3&4				
Race				
White	N/A		N/A	
Other				
miR-429				
Low	1.522 (1.004-2.307)	0.048	1.818 (1.104-2.993)	0.019
High	Reference		Reference	

Abbreviation: CI, confidence interval; HR, hazard ratio; OS, overall survival; DFS, disease free survival.

MiR-429 Suppresses the Proliferation, Invasion, and Migration of the PDAC Cancer Cell Line Bxpc-3

Next, whether miR-429 exerted tumor-suppressive effect on PDAC cells was investigated *via* transfection of a miR-429 mimic into Bxpc-3 cells. The expression of miR-429 was found to be upregulated in the transfected Bxpc-3 cells (Figure 4A). Cell proliferation was subsequently measured using CCK-8 and SRB assays at 24, 48, and 72 h. As shown in Figure 4B-C, the overexpression of miR-429 significantly inhibited Bxpc-3 cell proliferation at 48 and 72 h compared with cells transfected with NC. The results of the migration and invasion assays also revealed that the overexpression of miR-429 significantly suppressed the migratory and invasive abilities of Bxpc-3 cells compared with cells transfected with NC (Figure 4D-E). The expression of miR-429 was subsequently knocked down by transfecting a miR-429

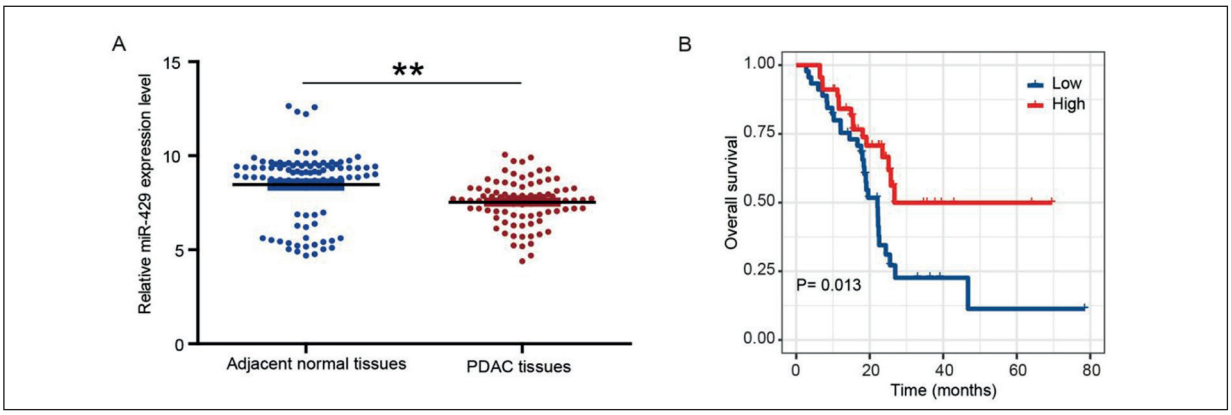

Figure 2. The expression and prognosis of miR-429 in 90 PDAC patients. **A, B,** The expression (**A**) (paired *t*-test) and prognosis (**B**) of miR-429 in 90 PDAC patients. The Kaplan-Meier method was used to draw survival curves, and the log-rank test was performed to evaluate survival difference with the best cut-off value. **, $p<0.01$.

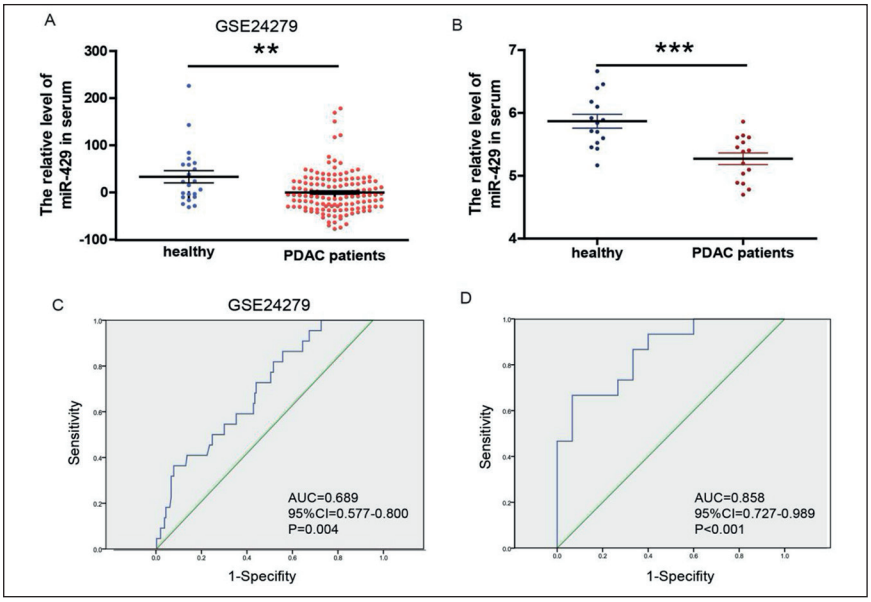

Figure 3. Serum miR-429 level is decreased in PDAC patients. **A,** The level of miR-429 in the serum of PDAC patients and healthy donors based on GSE24279 (unpaired *t*-test). **B,** The miR-429 level in the serum of 15 PDAC patients and 15 healthy donors (unpaired *t*-test). **C-D,** ROC analysis of miR-429 mRNA expression as a diagnostic marker in PDAC patients based on GSE24279 (**C**) and 15 PDAC patients and 15 healthy donors (**D**). **, $p<0.01$; ***, $p<0.001$.

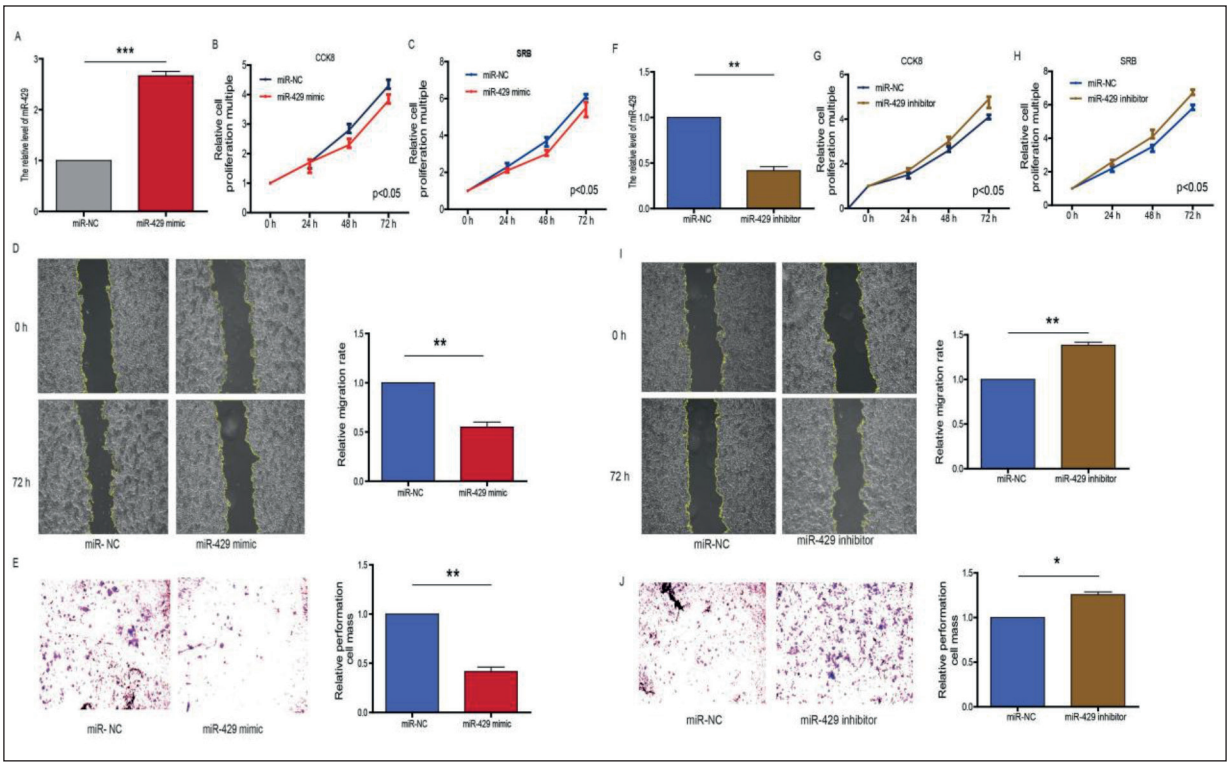

Figure 4. MiR-429 inhibited Bxpc-3 cells proliferation, migration and invasion. **A,** The level of miR-429 in Bxpc-3 cells were affected by transfection of miR-429 NC or mimics (paired *t*-test). **B-C,** The cellular proliferation was analyzed by CCK8 assay and SRB assay. **D,** The migration ability of Bxpc-3 cells with miR-429 mimics or NC transfection (paired *t*-test). **E,** The invasion ability of Bxpc-3 cells with miR-429 mimics or NC transfection (paired *t*-test) (magnification ×50). **F,** The expression of miR-429 in Bxpc-3 cells were affected by transfection of miR-429 inhibitor or NC (paired *t*-test). **G-H,** CCK8 and SRB assay were used to evaluate the proliferation of Bxpc-3 cells following transfection with miR-429 inhibitor or NC. **I,** The migration ability of Bxpc-3 cells with miR-429 inhibitor or NC transfection (paired *t*-test). **J,** The invasion ability of Bxpc-3 cells with miR-429 inhibitor or NC transfection (paired *t*-test). Relative quantification of miR-429 expression were calculated with the $2^{-\Delta\Delta Ct}$ method (magnification ×50). Paired *t*-test: *, $p<0.05$; **, $p<0.01$; ***, $p<0.001$.

inhibitor into Bxpc-3 cells, and RT-qPCR analysis subsequently confirmed that the miR-429 inhibitor was able to downregulate miR-429 expression (Figure 4F). As shown in Figure 4G-H, the knockdown miR-429 expression significantly promoted Bxpc-3 cell proliferation at 48 and 72 hours, and significantly promoted the migratory and invasive abilities of Bxpc-3 cells compared with cells transfected with NC (Figure 4G-J).

Identification of MiR-429 Target Genes in PDAC

To identify the modules of co-expressed genes that were negatively correlated with miR-429 expression, WGCNA based on the TCGA database was performed (Figure 5A-C). The network topology for soft-thresholding powers from 1 to 30 was also calculated to select the optimum threshold. One of the most critical parameters in

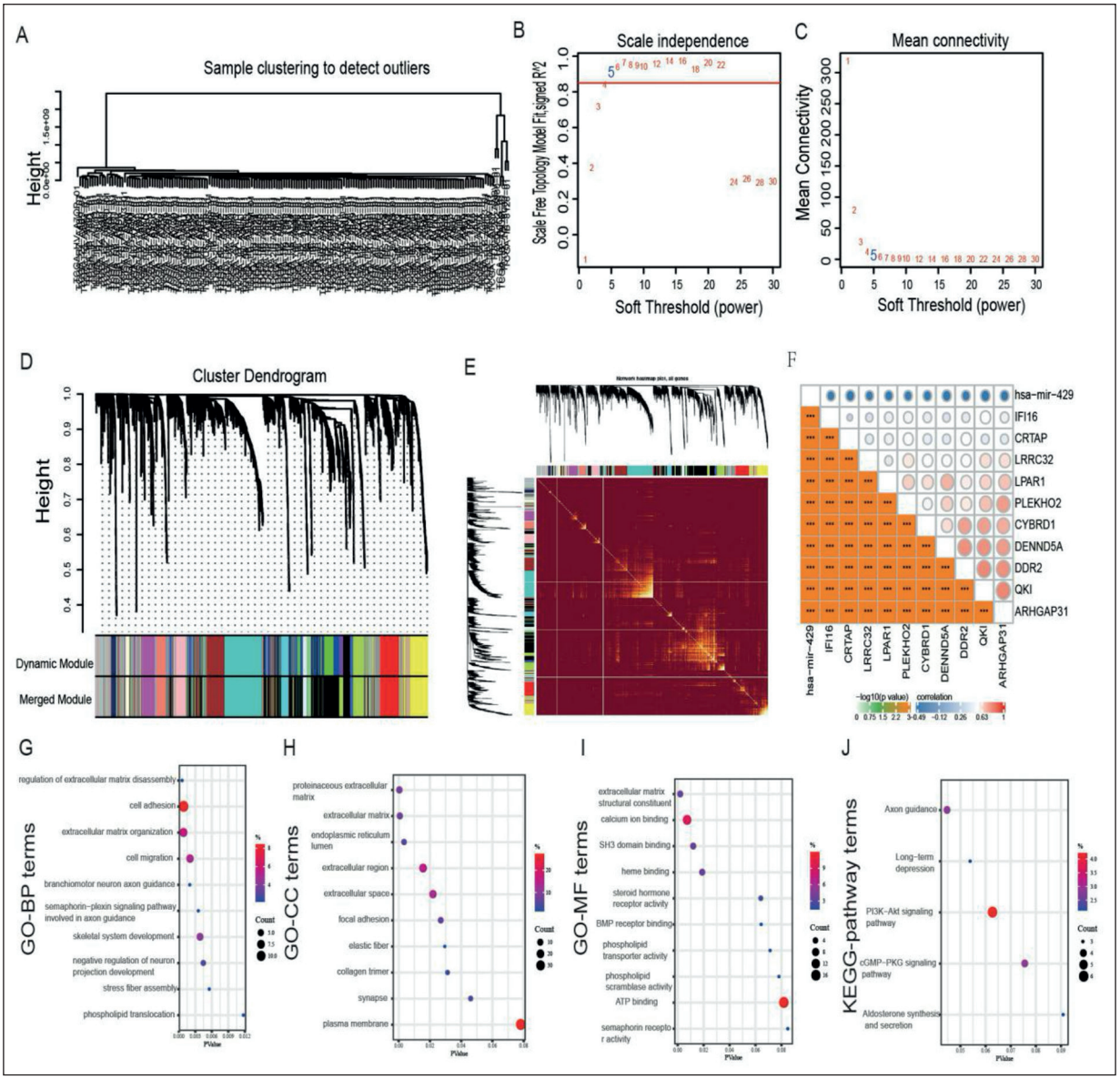

Figure 5. Identification of co-expression module genes associated with miR-429 in PDAC using the WGCNA. **A,** Clustering dendrogram of PDAC tissues. **B,** Relationship between scale-free topology model fit and soft-thresholds (powers). **C,** Relationship between the mean connectivity and various soft thresholds. **D,** Dendrogram of modules identified by WGCNA. **E,** Topological overlap matrix among detected genes from RNAseq. **F,** Top 10 red model genes negative correlated with miR-429 expression in PDAC. **G-J,** GO-BP (**G**), GO-CC (**H**), GO-MF (**I**) and KEGG pathway (**J**) analysis for the target genes in red model.

the WGCNA network construction is the power value, which affects the average connectivity and independence of each co-expression module. A power value of 3 was the lowest power for the scale-free topology. The co-expression similarity matrix was transformed into an adjacency matrix, and the TOM was calculated. The dynamic tree cut analysis gave rise to 18 modules with different colors (Figure 5D-E).

Next, Spearman's correlation analysis was used to determine the correlation between the identified target genes and miR-429 in PDAC tissues using the TCGA database. The top 10 negatively correlated genes are shown in Figure 5F. Based on the correlation coefficient with the threshold value of ($r < -0.3$), 129 genes were identified to be negatively correlated with miR-429. Among them, the highest percentages were found in the red module, with 44.9% of the 129 genes. To gain further insights into the function of the genes in the red module, GO functional term and KEGG signaling pathway enrichment analyses were conducted the ing DAVID database (Figure 5G-J). The top 10 BP terms were 'regulation of extracellular matrix disassembly', 'cell adhesion', 'extracellular matrix organization', 'cell migration', 'branchiomotor neuron axon guidance', 'semaphorin-plexin signaling pathway involved in axon guidance', 'skeletal system development', 'negative regulation of neuron projection development', 'stress fiber assembly' and 'phospholipid translocation'. The enriched KEGG signaling pathway terms were 'axon guidance', 'long-term depression', 'PI3K-Akt signaling pathway', 'cGMP-PKG signaling pathway', 'aldosterone synthesis', and 'secretion'.

In addition, the GSE41369 dataset was also used to identify genes negatively correlated with miR-429 in PDAC tissues. The top 10 negatively correlated genes are shown in Figure 6A. The heat map and volcano plot presented in Figure 6B-C show the differentially expressed genes (DEGs) in PDAC tissues. Venn diagram analysis identified 1,071 overlapping genes between the DEGs and negatively correlated genes that were associated with miR-429 in the GSE41369 dataset (Figure 6D). The intersection of the Venn diagram between TCGA data and the GSE41369 dataset identified 28 genes with potential miR-429-mRNA interactions (Figure 6E).

Finally, the potential target genes of miR-429 were predicted using the target prediction databases, miRDB and TargetScan. Venn diagram analysis identified five overlapping genes between the 28 genes and the target prediction databases (Figure 7A): Cadherin 11 (CDH11), inositol polyphosphate-4-phosphatase type I (INPP4A), laminin γ1 (LAMC1), low density lipoprotein receptor-related protein 1 (LRP1) and QKI, KH domain containing RNA binding (QKI). The results obtained from the analysis of the GEPIA database revealed that CDH11, INPP4A, LAMC1, LRP1, and QKI expression levels were upregulated in PDAC tissues (Figure 7B-F). To explore the significance of these five genes in the clinical prognosis of PDAC, Kaplan-Meier survival analysis was used to construct OS and DFS curves for patients with PDAC. The Kaplan-Meier survival curve demonstrated that patients with PDAC with high CDH11 and QKI expression led to a shorter OS and DFS (Figure 7G-P), but the OS and DFS of patients were not related to INPP4A, LAMC1 and LRP1 expression (Figure 7H-J and 7M-O). Detailed gene expression and clinical information for 174 PDAC patients in the TCGA database were presented in the **Supplementary Table IV**. The expression of CDH11 and QKI was also found to be upregulated in PDAC tissues obtained from the GSE60979, GSE71989, and GSE91035 datasets (Figure 7Q-V). Further analyses revealed that CDH11 and QKI expression could be downregulated by the overexpression of miR-429 in Bxpc-3 cells (Figure 8A-B). Finally, a prognostic nomogram was constructed to predict the survival of patients with PDAC based on the clinical factors of patients and miR-429, CDH1,1 and QKI expression (Figure 9A-B). The results revealed that patients with PDAC with upregulated expression of miR-429 and downregulated expression of CDH1 and QKI had a more favorable prognosis.

Discussion

Although significant improvements have been achieved in the treatment of several types of malignant tumors, in addition to advances in the understanding of cancer pathogenesis in recent decades, the outcomes of patients with PDAC remain elusive. Patients with PDAC often have an extremely poor survival outcome as only 15-20% of all patients are diagnosed at an early enough stage to be eligible for surgical resection[27-29]. Therefore, further research into the pathogenesis of PDAC is required to provide a theoretical basis for effective PDAC therapies. In addition, various miRNAs have been identified as prognostic

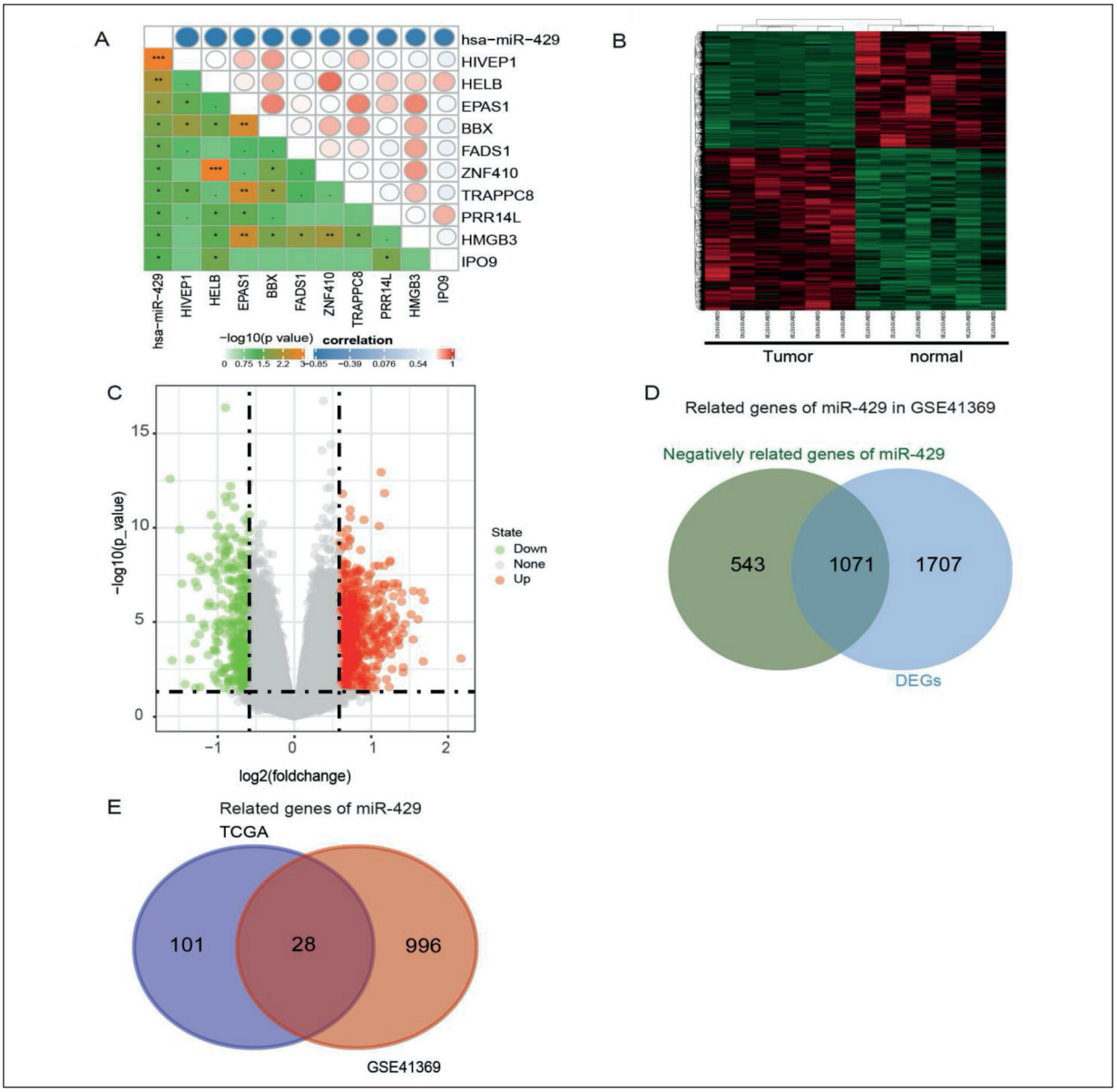

Figure 6. Identification of candidate miR-429 targeted genes in PDAC. **A,** Top 10 genes negative correlated with miR-429 expression in PDAC from GSE41369 database. **B-C,** Heatmap (**B**) and volcano plot (**C**) of The DEGs between PDAC tissuess and normal tissues from GSE41369 database. **D,** The overlap between negative correlated genes with miR-429 and DEGs was identified using a Venn diagram. **E,** The overlap between negative correlated genes with miR-429 in TCGA and GSE41369 was identified using a Venn diagram.

biomarkers, and several mechanisms considered to underlie the pathogenesis of PDAC have been studied. Previous studies have reported that miRNAs functioned as either tumor suppressors or oncogenes in tumor progression.

Accumulating evidence has indicated that the dysregulation of miR-429 expression, a member of the miR-200 family, may be involved in the progression of various types of cancer. For example, miR-429 expression levels were found to be downregulated in nephroblastoma[30], thyroid cancer[31], osteosarcoma[32,33], glioblastoma multiforme (GBM), and gastric cancer[34]. In nephroblastoma, miR-429 was discovered to inhibit cell proliferation by targeting c-Myc[30]. In addition, miR-429 was found to inhibit thyroid cancer

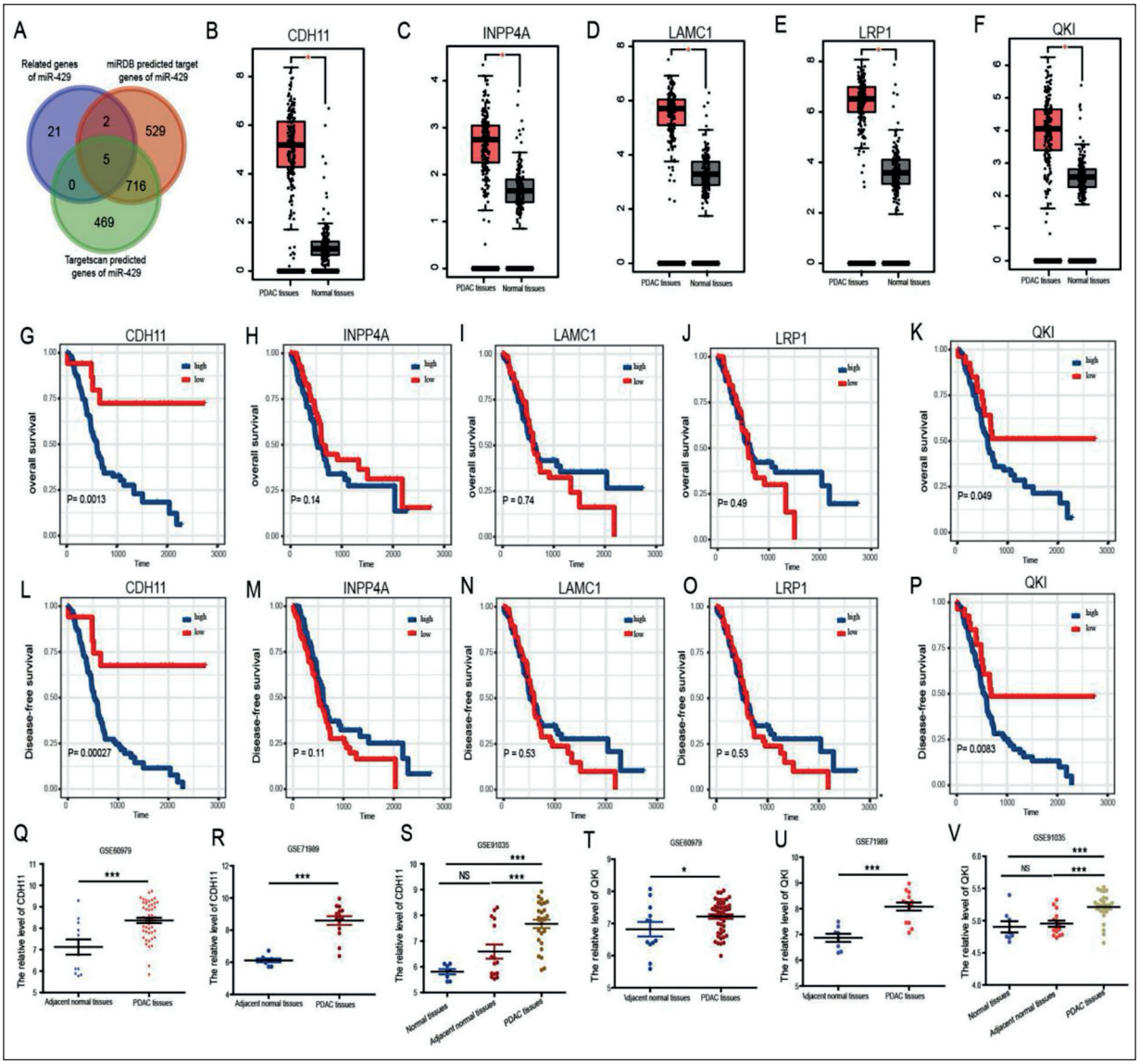

Figure 7. Expression and prognostic analysis of miR-429 target genes in PDAC. **A,** The overlap between negative correlated genes with miR-429, miRDB predicted target genes of miR-429 and Targetscan predicted target genes of miR-429 was identified using a Venn diagram. **B-F,** The expression levels of CDH11 (**B**), INPP4A (**C**), LAMC1 (**D**), LRP1 (**E**) and QKI (**F**) obtained from the GEPIA database (unpaired *t*-test). **G-K,** The OS analysis of CDH11 (**G**), INPP4A (**H**), LAMC1 (**I**), LRP1 (**J**) and QKI (**K**) in PDAC. **L-P,** The DFS analysis of CDH11 (**L**), INPP4A (**M**), LAMC1 (**N**), LRP1 (**O**) and QKI (**P**) in PDAC. **Q-S,** The expression of CDH11 in PDAC from GSE60979 (**Q**) (unpaired *t*-test), GSE71989 (R) (unpaired *t*-test) and GSE91035 (**S**) (One-way ANOVA). **T-V,** The expression of QKI in PDAC from GSE60979 (**T**) (unpaired t-test), GSE71989 (**U**) (unpaired t-test) and GSE91035 (**V**) (one-way ANOVA). The Kaplan-Meier method was used to draw survival curves, and the log-rank test was performed to evaluate survival difference with the best cut-off value. *, $p<0.05$. ***, $p<0.001$; NS, $p>0.05$.

cell proliferation and target zinc finger E-box binding homeobox 1 (ZEB1)[31]. In osteosarcoma, miR-429 was shown to inhibit the proliferation of osteosarcoma cells by targeting homeobox A9 (HOXA9) and ZEB1[32]. Furthermore, the expression of miR-429 was reported to be upregulated in non-small cell LC (NSCLC)[15] and prostate cancer (PC)[35]. MiR-429 was also demonstrated to promote cell proliferation by targeting p27Kip1 in PC[35].

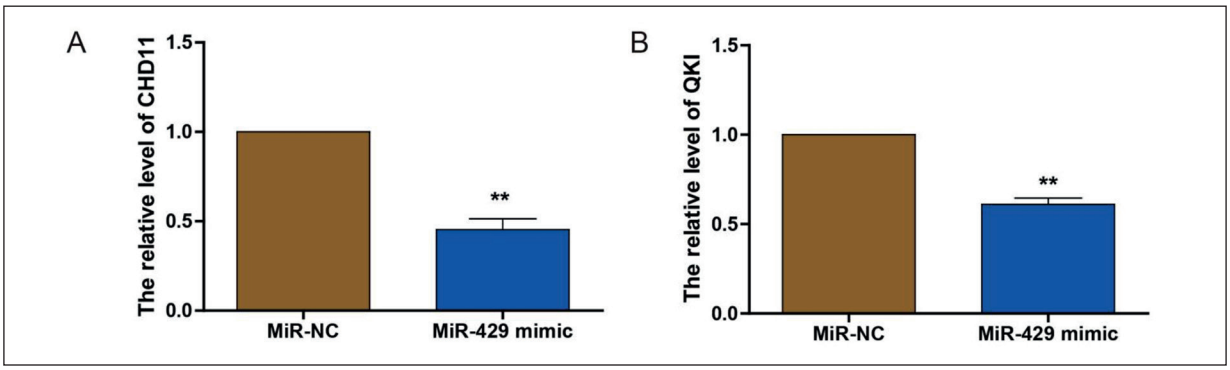

Figure 8. MiR-429 overexpression inhibits CDH11 and QKI expression. **A, B,** Effects of miR-429 on the (**A**) CDH11 and (**B**) QKI expression in Bxpc-3 cells.

The results of the present study revealed that the expression of miR-429 was downregulated in PDAC tissues compared with those in adjacent non-tumor tissues. In addition, decreased levels of miR-429 were also observed in the serum of patients with PDAC compared with those in healthy volunteers, suggesting that miR-429 may serve as a serum diagnostic marker in PDAC.

Next, miR-429 was discovered to suppress PDAC cell proliferation, invasion, and migration, which supports its potential tumor suppressive role in PDAC. MiRNAs exert their effects by inhibiting the expression of multiple target mRNAs. For example, miR-429 was reported to inhibit the proliferation of osteosarcoma cells by targeting HOXA9 and ZEB1[32,33]. Therefore, miR-429 may exert its effects by targeting multiple mRNAs in PDAC. Based on WGCNA, correlation analysis and target gene database prediction (TargetScan and miRDB), five genes (CDH11, INPP4A, LAMC1, LRP1 and QKI) were predicted to be target genes of miR-429 in PDAC. Previous studies[36,37] have reported that the aberrant expression of CDH11 influenced invasion and metastasis in a variety of tumor types. CDH11 has also been reported to be involved in several signaling pathways. For instance, CDH11 was found to be involved in epithelial-mesenchymal transition (EMT) by affecting the STAT3 signaling pathway, and it also regulated the WNT signaling pathway by regulating β-catenin[38,39]. QKI is an RNA-binding protein of the signal transduction

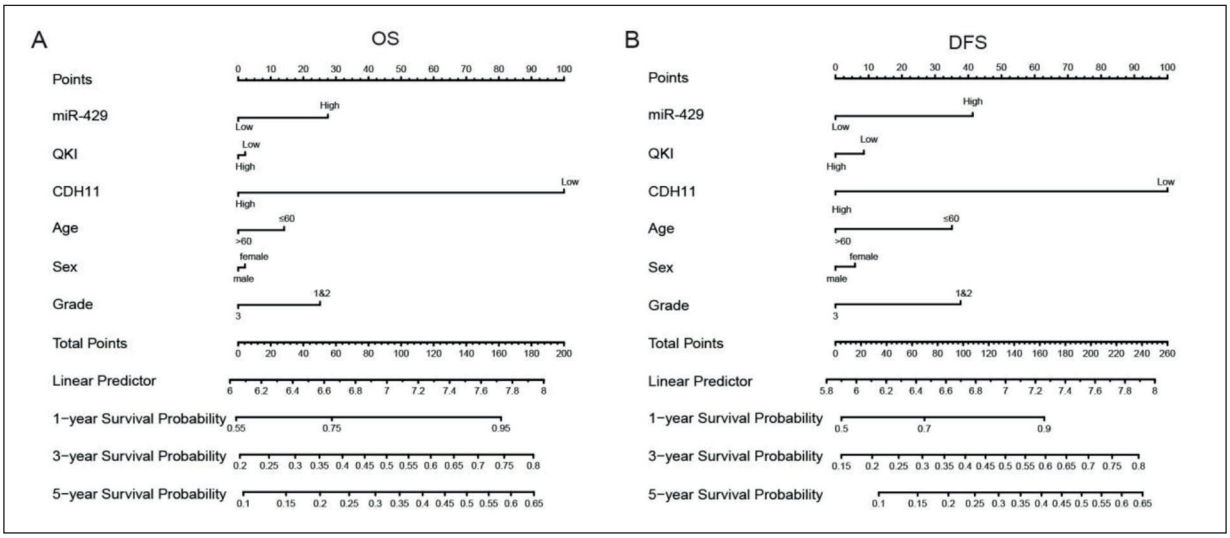

Figure 9. Prognostic nomogram based on miR-429, CDH11 and QKI in PDAC**. A, B,** The nomogram to predict OS (**A**) and DFS (**B**) were created based on miR-429, CDH11 and QKI in PDAC.

and activation of the RNA family that regulates mRNA splicing and stabilization, and circular RNA formation[40,41]. QKI has been reported to act as a tumor suppressor by inhibiting the EMT pathway in LC[42]. However, a more recent report[43] has shown that QKI promoted EMT *via* the modulation of alternative splicing in breast cancer. These opposing effects of QKI may be dependent on the cellular context in each type of cancer[44]. INPP4A is a magnesium-dependent phosphatase that has been discovered to play an important role in the metabolism of inositol[45,46]. A previous study[47] reported that the knockdown of INPP4A increased the proliferation, migration, and invasion of bladder cancer cells. LAMC1 encodes the laminin γ1 chain, which is the most common γ subunit of laminins and has been implicated to play an important role in various types of tumor[48]. The upregulated expression of LAMC1 was also found to be associated with the poor prognosis of patients with hepatocellular carcinoma, glioma, and gastric cancer[48-50]. LRP1 is a large multifunctional endocytic cell surface receptor, this transmembrane receptor recognizes numerous ligands, thereby regulating a wide range of biological functions[51]. Several studies[52-54] have indicated that LRP1 may play an important role in the regulation of tumor growth and progression. The upregulated expression of LRP1 was found to be associated with advanced tumor stages in breast cancer and EmCa[52-54].

Next, we found that these genes were upregulated in PDAC, but only CDH11 and QKI were associated with the OS and DFS of patients with PDAC. Thus, CDH11 and QKI are highly likely to be target genes of miR-429 in PDAC. Previous studies[55,56] have found that the expression of CDH11 was upregulated in gastric cancer, breast cancer, and brain malignancy tissues compared with those in normal tissues. The knockdown of CDH11 was discovered to inhibit cell proliferation and metastasis in GBM and breast cancer[55]. Higher expression of QKI was also found to be associated with poor clinical outcomes in breast cancer[56]. Previous studies[57,58] have reported that CDH11 and QKI acted as tumor suppressor genes in several types of tumors. Therefore, the downregulated expression of miR-429 may upregulate the expression of CDH11 and QKI to facilitate the progression of PDAC and decrease the survival time of patients with PDAC.

The current study has two limitations. First, the number of healthy is disproportionate to the number of PDAC patients, especially for GSE24279. Second, the number of patients that serum was collected from was relatively small. However, these results provide a preliminary indication of the role of miR-429 in PDAC and suggest that several miR-429 target genes may have potential as biomarkers for the clinical diagnosis of PDAC.

Conclusions

The findings of the present study indicated that the expression levels of miR-429 may be downregulated in both tumor tissues and the serum of patients with PDAC. Further experimental assays revealed that miR-429 suppressed the proliferation, invasion, and migration of PDAC cells. CDH11 and QKI were also identified as likely target genes of miR-429.

Conflict of Interest

The Authors declare that they have no conflict of interests.

Acknowledgements

Not applicable.

Funding

This research was funded by Cultivating Program for Young and Middle-Aged Talents of Fujian Provincial Health Commission (2017-ZQN-11).

Authors' Contribution

Wentao Huang, Tiansheng Lin and Junyi Wu wrote the main manuscript text. Wentao Huang, Tiansheng Lin, Junyi Wu and Jiaming Hong prepared figures 1-4. Wentao Huang, Jiaming Hong, Yiling Chen and Funan Qiu prepared figures 5-9. All authors have agreed on the journal to which the article will be submitted, gave final approval of the version to be published, and agree to be accountable for all aspects of the work.

Ethics Approval and Consent to Participate

The study was approved by the Ethics Committee of the Fujian Provincial Hospital and complied with the Helsinki Declaration (approval No. K2014-11-029). Written consent was obtained from all study participants.

Consent for Publication

Not applicable.

Availability of Data and Materials

The datasets used and/or analyzed during the current study are available from the corresponding author on reasonable request.

References

1) Philip PA, Mooney M, Jaffe D, Eckhardt G, Moore M, Meropol N, Emens L, O'Reilly E, Korc M, Ellis L, Benedetti J, Rothenberg M, Willett C, Tempero M, Lowy A, Abbruzzese J, Simeone D, Hingorani S, Berlin J, Tepper J. Consensus report of the national cancer institute clinical trials planning meeting on pancreas cancer treatment. J Clin Oncol 2009; 27: 5660-5669.
2) Conroy T, Desseigne F, Ychou M, Bouché O, Guimbaud R, Bécouarn Y, Adenis A, Raoul JL, Gourgou-Bourgade S, de la Fouchardière C, Bennouna J, Bachet JB, Khemissa-Akouz F, Péré-Vergé D, Delbaldo C, Assenat E, Chauffert B, Michel P, Montoto-Grillot C, Ducreux M. FOLFIRINOX versus gemcitabine for metastatic pancreatic cancer. N Engl J Med 2011; 364: 1817-1825.
3) Nagata N, Kawazoe A, Mishima S, Wada T, Shimbo T, Sekine K, Watanabe K, Imbe K, Kojima Y, Kumazawa K, Mihara F, Tokuhara M, Edamoto Y, Igari T, Yanase M, Mizokami M, Akiyama J, Uemura N. Development of Pancreatic Cancer, Disease-specific Mortality, and All-Cause Mortality in Patients with Nonresected IPMNs: A Long-term Cohort Study. Radiology 2016; 278: 125-134.
4) Zeitouni D, Pylayeva-Gupta Y, Der CJ, Bryant KL. KRAS Mutant Pancreatic Cancer: No Lone Path to an Effective Treatment. Cancers (Basel) 2016; 8.
5) Siegel RL, Miller KD, Jemal A. Cancer statistics, 2016. CA Cancer J Clin 2016; 66: 7-30.
6) Deplanque G, Demarchi M, Hebbar M, Flynn P, Melichar B, Atkins J, Nowara E, Moyé L, Piquemal D, Ritter D, Dubreuil P, Mansfield CD, Acin Y, Moussy A, Hermine O, Hammel P. A randomized, placebo-controlled phase III trial of masitinib plus gemcitabine in the treatment of advanced pancreatic cancer. Ann Oncol 2015; 26: 1194-1200.
7) Xiao R, Wang H, Yang B. MicroRNA-98-5p modulates cervical cancer progression via controlling PI3K/AKT pathway. Bioengineered 2021; 12: 10596-10607.
8) Ali Syeda Z, Langden SSS, Munkhzul C, Lee M, Song SJ. Regulatory Mechanism of MicroRNA Expression in Cancer. Int J Mol Sci 2020; 21.
9) Wang JK, Wang Z, Li G. MicroRNA-125 in immunity and cancer. Cancer Lett 2019; 454: 134-145.
10) Ow SH, Chua PJ, Bay BH. miR-149 as a Potential Molecular Target for Cancer. Curr Med Chem 2018; 25: 1046-1054.
11) Zhang L, Liu Q, Mu Q, Zhou D, Li H, Zhang B, Yin C. MiR-429 suppresses proliferation and invasion of breast cancer via inhibiting the Wnt/β-catenin signaling pathway. Thorac Cancer 2020; 11: 3126-3138.
12) Zong M, Liu Y, Zhang K, J Y, Chen L. The effects of miR-429 on cell migration and invasion by targeting Slug in esophageal squamous cell carcinoma. Pathol Res Pract 2019; 215: 152526.
13) Dong H, Hao X, Cui B, Guo M. MiR-429 suppresses glioblastoma multiforme by targeting SOX2. Cell Biochem Funct 2017; 35: 260-268.
14) Yoneyama K, Ishibashi O, Kawase R, Kurose K, Takeshita T. miR-200a, miR-200b and miR-429 are onco-miRs that target the PTEN gene in endometrioid endometrial carcinoma. Anticancer Res 2015; 35: 1401-1410.
15) Xiao P, Liu W, Zhou H. miR-429 promotes the proliferation of non-small cell lung cancer cells via targeting DLC-1. Oncol Lett 2016; 12: 2163-2168.
16) Oken MM, Creech RH, Tormey DC, Horton J, Davis TE, McFadden ET, Carbone PP. Toxicity and response criteria of the Eastern Cooperative Oncology Group. Am J Clin Oncol 1982; 5: 649-655.
17) Frampton AE, Castellano L, Colombo T, Giovannetti E, Krell J, Jacob J, Pellegrino L, Roca-Alonso L, Funel N, Gall TM, De Giorgio A, Pinho FG, Fulci V, Britton DJ, Ahmad R, Habib NA, Coombes RC, Harding V, Knösel T, Stebbing J, Jiao LR. MicroRNAs cooperatively inhibit a network of tumor suppressor genes to promote pancreatic tumor growth and progression. Gastroenterology 2014; 146: 268-277.
18) Sandhu V, Bowitz Lothe IM, Labori KJ, Skrede ML, Hamfjord J, Dalsgaard AM, Buanes T, Dube G, Kale MM, Sawant S, Kulkarni-Kale U, Børresen-Dale AL, Lingjærde OC, Kure EH. Differential expression of miRNAs in pancreatobiliary type of periampullary adenocarcinoma and its associated stroma. Mol Oncol 2016; 10: 303-316.
19) Sandhu V, Bowitz Lothe IM, Labori KJ, Lingjærde OC, Buanes T, Dalsgaard AM, Skrede ML, Hamfjord J, Haaland T, Eide TJ, Børresen-Dale AL, Ikdahl T, Kure EH. Molecular signatures of mRNAs and miRNAs as prognostic biomarkers in pancreatobiliary and intestinal types of periampullary adenocarcinomas. Mol Oncol 2015; 9: 758-771.
20) Jiang J, Azevedo-Pouly AC, Redis RS, Lee EJ, Gusev Y, Allard D, Sutaria DS, Badawi M, Elgamal OA, Lerner MR, Brackett DJ, Calin GA, Schmittgen TD. Globally increased ultraconserved noncoding RNA expression in pancreatic adenocarcinoma. Oncotarget 2016; 7: 53165-53177.
21) Sutaria DS, Jiang J, Azevedo-Pouly ACP, Lee EJ, Lerner MR, Brackett DJ, Vandesompele J, Mestdagh P, Schmittgen TD. Expression Profiling Identifies the Noncoding Processed Transcript of HNRNPU with Proliferative Properties in Pancreatic Ductal Adenocarcinoma. Non-coding RNA 2017; 3.
22) Bauer AS, Keller A, Costello E, Greenhalf W, Bier M, Borries A, Beier M, Neoptolemos J, Büchler M, Werner J, Giese N, Hoheisel JD. Diagnosis of pancreatic ductal adenocarcinoma and chronic pancreatitis by measurement of microRNA abundance in blood and tissue. PLoS One 2012; 7.

23) Agarwal V, Bell GW, Nam JW, Bartel DP. Predicting effective microRNA target sites in mammalian mRNAs. Elife 2015; 4.

24) Tang Z, Li C, Kang B, Gao G, Li C, Zhang Z. GEPIA: a web server for cancer and normal gene expression profiling and interactive analyses. Nucleic Acids Res 2017; 45: 98-102.

25) Huang da W, Sherman BT, Lempicki RA. Systematic and integrative analysis of large gene lists using DAVID bioinformatics resources. Nat Protoc 2009; 4: 44-57.

26) Wang Q, Ye Y, Lin R, Weng S, Cai F, Zou M, Niu H, Ge L, Lin Y. Analysis of the expression, function, prognosis and co-expression genes of DDX20 in gastric cancer. Comput Struct Biotechnol J 2020; 18: 2453-2462.

27) Dinse GE, Lagakos SW. Nonparametric estimation of lifetime and disease onset distributions from incomplete observations. Biometrics 1982; 38: 921-932.

28) Brooks J, Fleischmann-Mundt B, Woller N, Niemann J, Ribback S, Peters K, Demir IE, Armbrecht N, Ceyhan GO, Manns MP, Wirth TC, Kubicka S, Bernhardt G, Smyth MJ, Calvisi DF, Gürlevik E, Kühnel F. Perioperative, Spatiotemporally Coordinated Activation of T and NK Cells Prevents Recurrence of Pancreatic Cancer. Cancer Res 2018; 78: 475-488.

29) Ambe CM, Nguyen P, Centeno BA, Choi J, Strosberg J, Kvols L, Hodul P, Hoffe S, Malafa MP. Multimodality Management of "Borderline Resectable" Pancreatic Neuroendocrine Tumors: Report of a Single-Institution Experience. Cancer control 2017; 24: 1073274817729076.

30) Wang HF, Wang WH, Zhuang HW, Xu M. MiR-429 regulates the proliferation and apoptosis of nephroblastoma cells through targeting c-myc. Eur Rev Med Pharmacol Sci 2018; 22: 5172-5179.

31) Wu G, Zheng H, Xu J, Guo Y, Zheng G, Ma C, Hao S, Liu X, Chen H, Wei S, Song X, Wang X. miR-429 suppresses cell growth and induces apoptosis of human thyroid cancer cell by targeting ZEB1. Artif Cells Nanomed Biotechnol 2019; 47: 548-554.

32) Sun L, Wang L, Luan S, Jiang Y, Wang Q. miR-429 inhibits osteosarcoma progression by targeting HOXA9 through suppressing Wnt/β-catenin signaling pathway. Oncol Lett 2020; 20: 2447-2455.

33) Deng Y, Luan F, Zeng L, Zhang Y, Ma K. MiR-429 suppresses the progression and metastasis of osteosarcoma by targeting ZEB1. EXCLI J 2017; 16: 618-627.

34) Zhu P, Zhang J, Zhu J, Shi J, Zhu Q, Gao Y. MiR-429 Induces Gastric Carcinoma Cell Apoptosis Through Bcl-2. Cell Physiol Biochem 2015; 37: 1572-1580.

35) Ouyang Y, Gao P, Zhu B, Chen X, Lin F, Wang X, Wei J, Zhang H. Downregulation of microRNA-429 inhibits cell proliferation by targeting p27Kip1 in human prostate cancer cells. Mol Med Rep 2015; 11: 1435-1441.

36) Huang CF, Lira C, Chu K, Bilen MA, Lee YC, Ye X, Kim SM, Ortiz A, Wu FL, Logothetis CJ, Yu-Lee LY, Lin SH. Cadherin-11 increases migration and invasion of prostate cancer cells and enhances their interaction with osteoblasts. Cancer Res 2010; 70: 4580-4589.

37) Chu K, Cheng CJ, Ye X, Lee YC, Zurita AJ, Chen DT, Yu-Lee LY, Zhang S, Yeh ET, Hu MC, Logothetis CJ, Lin SH. Cadherin-11 promotes the metastasis of prostate cancer cells to bone. Mol Cancer Res 2008; 6: 1259-1267.

38) Satriyo PB, Bamodu OA, Chen JH, Aryandono T, Haryana SM, Yeh CT, Chao TY. Cadherin 11 Inhibition Downregulates β-catenin, Deactivates the Canonical WNT Signalling Pathway and Suppresses the Cancer Stem Cell-Like Phenotype of Triple Negative Breast Cancer. J Clin Med 2019; 8: 148.

39) Geletu M, Arulanandam R, Chevalier S, Saez B, Larue L, Feracci H, Raptis L. Classical cadherins control survival through the gp130/Stat3 axis. Biochim biophys Acta 2013; 1833: 1947-1959.

40) Chen AJ, Paik JH, Zhang H, Shukla SA, Mortensen R, Hu J, Ying H, Hu B, Hurt J, Farny N, Dong C, Xiao Y, Wang YA, Silver PA, Chin L, Vasudevan S, Depinho RA. STAR RNA-binding protein Quaking suppresses cancer via stabilization of specific miRNA. Genes Dev 2012; 26: 1459-1472.

41) Conn SJ, Pillman KA, Toubia J, Conn VM, Salmanidis M, Phillips CA, Roslan S, Schreiber AW, Gregory PA, Goodall GJ. The RNA binding protein quaking regulates formation of circRNAs. Cell 2015; 160: 1125-1134.

42) Zong FY, Fu X, Wei WJ, Luo YG, Heiner M, Cao LJ, Fang Z, Fang R, Lu D, Ji H, Hui J. The RNA-binding protein QKI suppresses cancer-associated aberrant splicing. PLoS Genet 2014; 10.

43) Pillman KA, Phillips CA, Roslan S, Toubia J, Dredge BK, Bert AG, Lumb R, Neumann DP, Li X, Conn SJ, Liu D, Bracken CP, Lawrence DM, Stylianou N, Schreiber AW, Tilley WD, Hollier BG, Khew-Goodall Y, Selth LA, Goodall GJ, Gregory PA. miR-200/375 control epithelial plasticity-associated alternative splicing by repressing the RNA-binding protein Quaking. EMBO J 2018; 37.

44) Kim EJ, Kim JS, Lee S, Lee H, Yoon JS, Hong JH, Chun SH, Sun S, Won HS, Hong SA, Kang K, Jo JY, Choi M, Shin DH, Ahn YH, Ko YH. QKI, a miR-200 target gene, suppresses epithelial-to-mesenchymal transition and tumor growth. Int J Cancer 2019; 145: 1585-1595.

45) Sharma M, Batra J, Mabalirajan U, Sharma S, Nagarkatti R, Aich J, Sharma SK, Niphadkar PV, Ghosh B. A genetic variation in inositol polyphosphate 4 phosphatase a enhances susceptibility to asthma. Am J Respir Crit Care Med 2008; 177: 712-719.

46) Wang L, Wang Y, Duan C, Yang Q. Inositol phosphatase INPP4A inhibits the apoptosis of in vitro neurons with characteristic of intractable epilepsy

by reducing intracellular Ca(2+) concentration. Int J Clin Exp Pathol 2018; 11: 1999-2007.

47) Wang R, Wu Y, Huang W, Chen W. MicroRNA-940 Targets INPP4A or GSK3β and Activates the Wnt/β-Catenin Pathway to Regulate the Malignant Behavior of Bladder Cancer Cells. Oncol Res 2018; 26: 145-155.

48) Liu J, Liu D, Yang Z, Yang Z. High LAMC1 expression in glioma is associated with poor prognosis. Onco Targets Ther 2019; 12: 4253-4260.

49) Han ZR, Jiang XL, Fan WC. LAMC1 is related to the poor prognosis of patients with gastric cancer and facilitates cancer cell malignancies. Neoplasma 2021; 68: 711-718.

50) Zhang Y, Xi S, Chen J, Zhou D, Gao H, Zhou Z, Xu L, Chen M. Overexpression of LAMC1 predicts poor prognosis and enhances tumor cell invasion and migration in hepatocellular carcinoma. J Cancer 2017; 8: 2992-3000.

51) Boulagnon-Rombi C, Schneider C, Leandri C, Jeanne A, Grybek V, Bressenot AM, Barbe C, Marquet B, Nasri S, Coquelet C, Fichel C, Bouland N, Bonnomet A, Kianmanesh R, Lebre AS, Bouché O, Diebold MD, Bellon G, Dedieu S. LRP1 expression in colon cancer predicts clinical outcome. Oncotarget 2018; 9: 8849-8869.

52) Catasús L, Llorente-Cortés V, Cuatrecasas M, Pons C, Espinosa I, Prat J. Low-density lipoprotein receptor-related protein 1 (LRP-1) is associated with highgrade, advanced stage and p53 and p16 alterations in endometrial carcinomas. Histopathology 2011; 59: 567-571.

53) Catasus L, Gallardo A, Llorente-Cortes V, Escuin D, Muñoz J, Tibau A, Peiro G, Barnadas A, Lerma E. Low-density lipoprotein receptor-related protein 1 is associated with proliferation and invasiveness in Her-2/neu and triple-negative breast carcinomas. Hum Pathol 2011; 42: 1581-1588.

54) McGarvey T, Hussain MM, Stearns ME. In situ hybridization studies of alpha 2-macroglobulin receptor and receptor-associated protein in human prostate carcinoma. Prostate 1996; 28: 311-317.

55) Wang Q, Jia Y, Peng X, Li C. Clinical and prognostic association of oncogene cadherin 11 in gastric cancer. Oncol Lett 2020; 19: 4011-4023.

56) Gu S, Chu C, Chen W, Ren H, Cao Y, Li X, He J, Wang Y, Jin Y, Liu X, Zou Q. Prognostic value of epithelial-mesenchymal transition related genes: SLUG and QKI in breast cancer patients. Int J Clin Exp Pathol 2019; 12: 2009-2021.

57) Wu L, Liu Y, Guo C, Shao Y. LncRNA OIP5-AS1 promotes the malignancy of pancreatic ductal adenocarcinoma via regulating miR-429/FOXD1/ERK pathway. Cancer Cell Int 2020; 20: 296.

58) Chen D, Zhao H. The inhibiting effects of microRNA-429 on the progression of pancreatic ductal adenocarcinoma cells by inhibiting epithelial mesenchymal transition. Am J Transl Res 2021; 13: 3286-3293.